METHODOLOGY FOR ENSURING SAFETY OF AN EMBARKED HELICOPTER SECURING SYSTEM PROBE INSTALLATION

R. Langlois*, P. Keary†
***Carleton University, Indal Technologies Inc., rlangloi@mae.carleton.ca;**
†Kaman Aerospace Corp., kearyp-kac@kaman.com

Keywords: *dynamic interface analysis, structural analysis, fatigue analysis, helicopter*

Abstract

Novel methodology is presented that combines dynamic interface analysis, detailed computational stress analysis and validation, full-scale destructive component assembly testing, and proof-load testing to ensure that the design and installation of the helicopter-mounted portion of the Indal Technologies Inc. Recovery Assist Secure and Traverse (RAST) system in the Kaman Aerospace Corp. SH-2G(A) Super Seasprite helicopter meets or exceeds safety and operational requirements for shipboard launch and recovery in severe sea conditions. The approach is outlined, followed by quantitative results and comprehensive discussion of each aspect of the project through to aircraft/probe substantiation testing. While the application of the methodology is specific, experience with the approach suggests that it is well suited for use in similar safety-critical applications.

1 Introduction

1.1 Background

A continuing trend towards routinely operating embarked helicopters from small ships in increasingly severe sea and wind conditions is motivating aircraft and securing equipment manufacturers to work closely together to analyze the systems involved and develop robust design methodologies that ensure efficient and safe designs.

A joint project was recently completed by Indal Technologies Inc. (ITI) and Kaman Aerospace Corp. (KAC) to integrate the aircraft-mounted portion of the ITI Recovery Assist Secure and Traverse (RAST) and Aircraft/Ship Integrated Secure and Traverse (ASIST) helicopter securing and handling systems with the KAC SH-2G(A) Super Seasprite helicopter, thereby allowing embarked operation of the SH-2G(A) in severe sea conditions. To achieve the objectives of this project, novel methodology was developed to fully exploit the thoroughness of simulation technology for defining the spectrum of dynamic loads acting on the aircraft, the efficiency of computational stress analysis for equipment design and optimization, and the realism of full-scale structural testing for characterizing actual 'as-built' hardware. The structural test data were reintegrated into the analysis to the extent possible, to assess the accuracy of stress analyses and to calibrate cycles-to-failure curves for use in subsequent cumulative damage fatigue analysis. The methodology provides an efficient design approach that tightly integrates the various methods and maximizes the safety of the resulting equipment installation.

The ITI RAST and ASIST securing systems use a ship-mounted rapid securing device (RSD) to positively engage an aircraft-mounted retractable probe that extends from the bottom of the aircraft. The systems facilitate landing helicopters by providing cues that guide the aircraft onto the deck such that the probe can be captured immediately upon touchdown by the RSD (typically within 2 seconds of landing). Once initially secured, the aircraft remains secured throughout all aspects of on-deck handling operations including straightening of

the aircraft, traversing it into the hangar, and subsequently throughout the entire launch sequence. The primary aircraft-mounted structural element in both systems is the retractable probe. Figure 1 shows a labelled schematic view of key RAST probe elements and the corresponding solid model used during its design. The two main structural elements are the housing, that is fabricated from aluminum alloy, and the probe shaft, that is fabricated from high strength stainless steel. The probe housing interfaces with the aircraft structure through upper and lower fittings with the housing isolated from the fittings by stiff polyurethane resilient rings. These resilient rings limit the shock load transmitted to the airframe during probe capture and on-deck securing. During securing and on-deck operation, the probe shaft is fully extended, thereby cantilevering the portion of the probe below the lower mount. When not in use, the probe shaft is retracted into the housing.

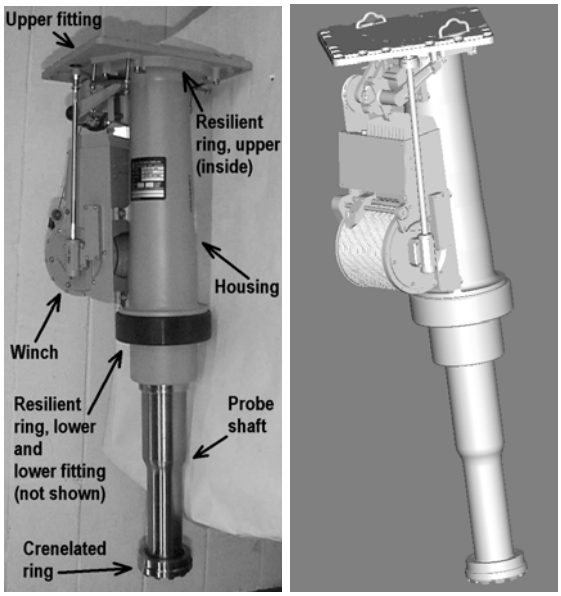

Figure 1. Annotated views of the RAST probe (left) and CAD model (right)

Figure 2 illustrates the interface between the probe and the RAST RSD. The main landing gear, auxiliary landing gear, and probe share forces that oppose sliding, yawing, and toppling of the aircraft. Clearance and controlled compliance between the probe shaft and the RSD beams (RAST) or claw (ASIST) result in probe forces only when they are required to supplement landing gear reaction forces in securing the aircraft. However, securing of the aircraft generates intermittent loading on the probe tip during all but the most benign sea conditions.

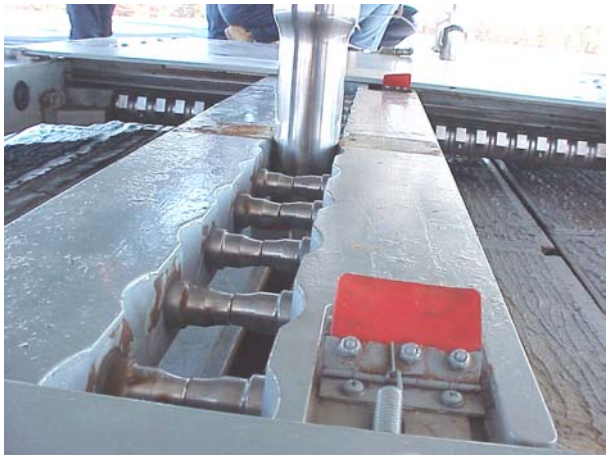

Figure 2. Pictorial view of the interface between the probe and RAST RSD

To integrate the securing system, KAC redesigned the lower fuselage of the SH-2G(A) to incorporate the probe. This is described in detail in Section 3.2

The continuous nature of probe loading, variability of loading conditions, potential magnitude of securing forces, and anticipated number of load cycles motivated detailed analysis of the static and fatigue safety of both the probe structural elements and the aircraft structure to which the probe is mounted and through which shipboard securing loads are transmitted.

1.2 Approach

The methodology for dynamic analysis, structural analysis, and testing was developed and used for integrating the securing system with the aircraft is presented schematically in Figure 3. This process is briefly described prior to the detailed discussion in subsequent sections.

The first essential step in the methodology was quantification of the dynamic loading acting on the probe, the landing gear, and consequently on

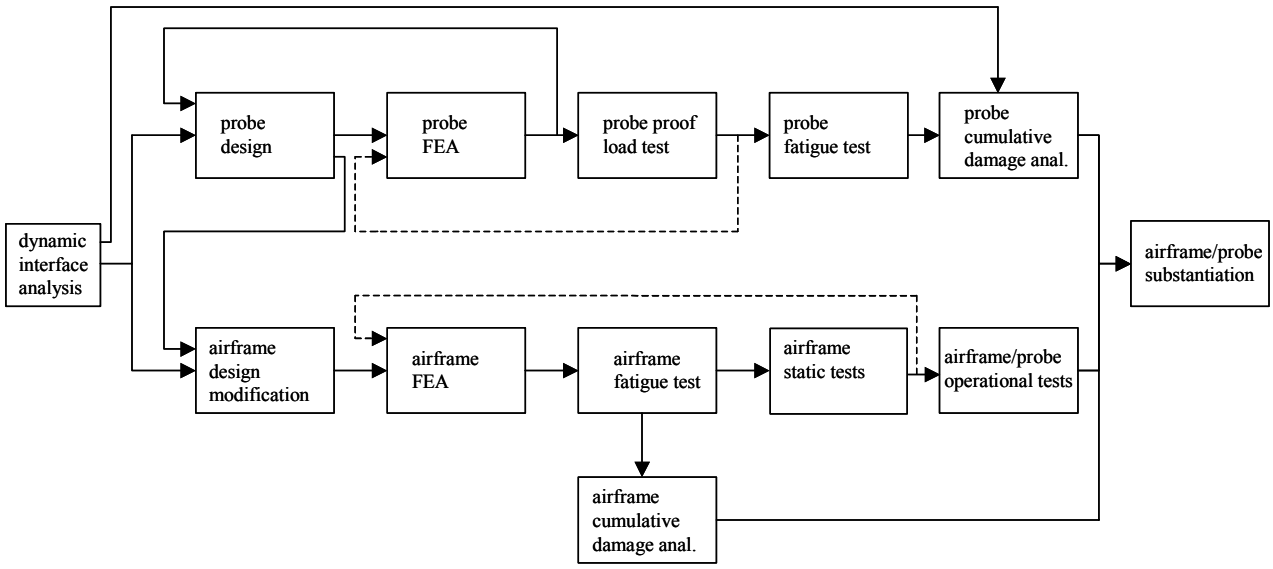

Figure 3. Overview of methodology developed for integrating the RAST probe with the SH-2G(A) Super Seasprite

the aircraft structure. The dynamic loading is dependent on three main factors: aircraft and securing system design in terms of geometrical, inertial, and stiffness parameters; sea conditions; and operational factors such as ship heading and speed relative to the principal sea direction. Detailed nonlinear transient dynamic simulation was ideal for this step as it provided a means of exploring the full parameter space prior to detailed design of the probe and aircraft systems. The simulation was used to generate securing force data of two types: peak securing load data for the complete range of operational conditions which lead to the peak static design loads; and time-domain data which was subsequently post-processed and lead to fatigue spectra based on a reduced set of representative operational cases.

The static and fatigue loads were then used for both probe design (upper path in Figure 3) and airframe modification (lower path in Figure 3). It is apparent that close similarity exists along the two paths. The simulation-based design loads were used for mechanical design that was supported by detailed finite element analyses. Load testing was performed on advanced development instrumented models of the actual hardware. Experimental data obtained from these static tests were used to validate and refine the finite element models. Fatigue testing was then performed using a loading ratio that was determined based on the simulation results. In the case of the destructive fatigues tests (such as the probe), loading was applied based on a block-loading approach to ensure expeditious but representative failure of the components and systems. In the latter case, fatigue test results were then used to calibrate cycles to failure curves. These were then combined with the simulated fatigue spectra to perform Palmgren-Minor cumulative damage analysis to estimate the fatigue life of the respective systems. Functional testing was performed on the airframe and probe systems individually. Finally, the completed airframe/probe system was substantiated based on mock service conditions.

2 Dynamic Interface Analysis

2.1 Simulation Methodology

Time histories of the forces and relative displacements that result from the dynamic interface between the SH-2G(A) and the specific frigate considered were developed using ITI's proprietary *Dynaface*® dynamic interface simulation software [1]. The simulation and associated analysis methodology

has evolved over the past twelve years and is currently used extensively for the analysis of dynamic interface issues. *Dynaface*® consists of a special-purpose 15-degree-of-freedom nonlinear transient-dynamic mathematical model of the aircraft/ship system. The model includes detailed representations of the oleo stiffness, damping, and friction characteristics; induced rotor forces; and a detailed tire model that supports complex tire behaviour including intermittent tire contact, rolling due to suspension travel, brake slippage, and sliding of the contact patch. For the purpose of this project, ship motion was generated using established linear strip theory [2].

2.2 Simulation conditions

The design goal for the probe for embarked securing was to maintain operability in all sea conditions up to upper sea state 5 and limited operability (in terms of ship heading) in sea state 6 [3].

The specific character and magnitude of the securing forces and corresponding landing gear reaction forces vary considerably with the specific phase of aircraft operation, aircraft configuration, and environmental conditions. Phases of on-deck aircraft operation include securing, manoeuvring, traversing, and hangaring. Aircraft configuration includes parameters such as aircraft mass, rotor status (stopped or turning), alignment with the ship centreline, and tire and oleo servicing factors. Environmental conditions include sea state, ship heading, ship speed, wind speed, wind direction, and geographic location. In service, an aircraft/probe system may operate in conditions characterized by all combinations of these parameters. This results in a very large number of possible operating conditions, each having an associated probability of occurrence.

As a result, dynamic analysis must consider a range of simulation conditions. Tables 1 and 2 present the simulation cases considered for the peak static loads and fatigue spectra analyses respectively.

Table 1. Simulation conditions used for peak loads analysis

Parameter	Value
Aircraft weight	10580 lbf, 13500 lbf
Rotor status	Stopped, turning
Brake status	Applied, not applied
Aircraft alignment	30°, 0°, +30°
Suspension parameters	Nominal
Ship speed	10, 15, 20, 25 knots
Ship headings	0° - 180° in 15° increments
Wind speed	35 knots
Wind direction	Port and starboard beam
Sea modal period	9.7 sec for SWH of 4 m 12.4 sec for SWH of 6 m
Ship motion criteria used to define severe deck conditions	Roll, pitch, 5 acceleration-based parameters

Table 2. Simulation conditions used for fatigue spectra analysis

Parameter	Value
Aircraft weight	13500 lbf
Rotor status	Turning
Aircraft alignment	Aligned with ship centreline
Suspension parameters	Nominal
Ship speed	10 knots
Ship headings	0°, 30°, 60°, 90°, 120°, 150°
Wind speed	19 knots for SWH of 2.5 m 24.5 knots for SWH of 4 m
Wind direction	Aligned with sea
Sea modal period	8.8 sec for SWH of 2.5 m 9.7 sec for SWH of 4 m 12.4 sec for SWH of 6 m

2.3 Peak securing and landing gear loads

From the peak loads simulation study [4], the peak static securing loads were determined to be 9.2 kips, 15.8 kips, 20.5 kips, and 16.3 kips in the longitudinal, lateral, vertical, and radial directions respectively, applied to the probe tip (expressed in an aircraft-fixed coordinate system). The radial direction corresponds to the resultant of the longitudinal and lateral force components. It should be noted that these loads do not occur simultaneously as peak longitudinal and peak lateral loads tend to occur out of phase with each other. The peak landing

gear reaction forces acting on the main landing gear were found to be 3.5 kips, 5.0 kips, and 21.8 kips in the longitudinal, lateral, and vertical directions respectively. The tail landing gear forces were found to be 0.5 kips, 2.7 kips, and 11.3 kips in the longitudinal, lateral, and vertical directions respectively. For brevity, only the peak loads are presented here. Reference 4 provides a detailed description of how the loads vary with environmental and operational conditions.

2.4 Fatigue load spectra

Three observations derived from the dynamic analysis influenced the approach used for developing the fatigue load spectra:

- longitudinal probe loading is much less severe in amplitude and frequency than loading in the lateral and vertical directions, and produces probe stresses at locations other than the critical fatigue locations;
- lateral probe forces dominate the in-plane probe loading in terms of magnitude and number of occurrences; and
- though vertical securing force magnitudes are high, because they result in purely tensile loading of the probe that is distributed over the entire cross-section of the probe, internal probe stresses resulting from vertical loading are low (less than approximately 6% of the total stress at the most highly stressed locations).

Considering these, the data analysis focused on the lateral force fatigue cycles, which were counted using the standard rainflow counting method described by ASTM 1049-85 [5]. Vertical securing forces were considered as secondary loading. Cycle counting was performed for each of the simulation cases considered and the equivalent numbers of fully reversed cycles occurring per hour of RAST operation were determined as a function of lateral force range. The results are presented graphically in Figure 4. The results indicate that fatigue damage is relatively low when the SWH is 2.5 meters compared with 4.0 meters and that fatigue damage is largely limited to headings between 60° and 120° (defined using a convention where 0° corresponds to head seas). In the restricted operational headings when the SWH is 6 metres the fatigue loading was found to be minimal. From the probabilities of occurrence of sea state and ship heading as well as the expected number of hours of RAST securing during the design life of the aircraft, the total number of expected fatigue cycles were calculated as a function of load amplitude. This resulted in the probe fatigue-loading spectrum.

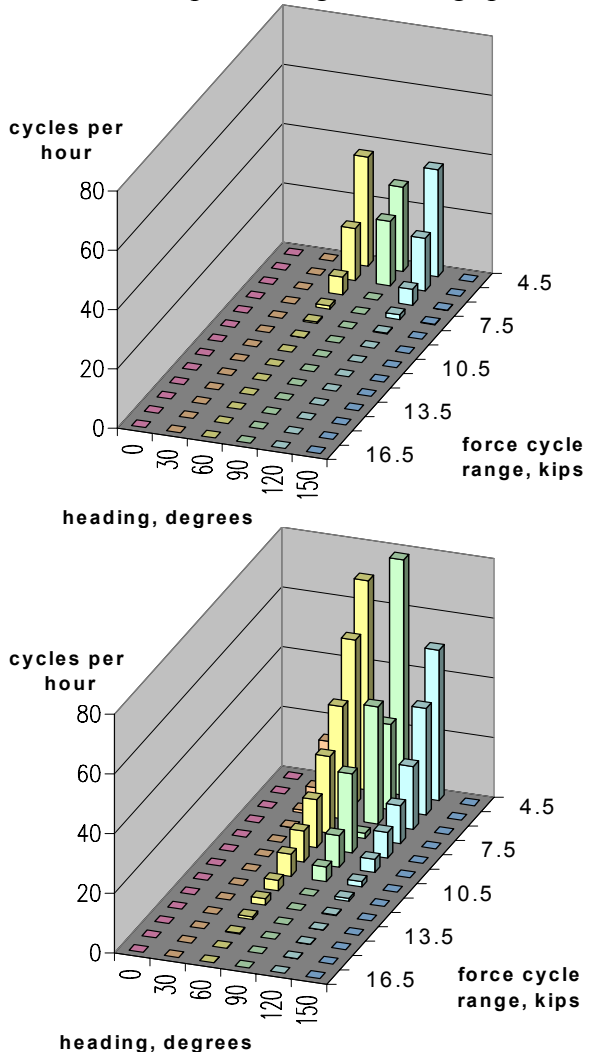

Figure 4. Distribution of fatigue cycles with wave height and ship heading for sea state 4 (top) and sea state 5 (bottom)

3 General description of airframe/probe support structure

3.1 SH-2G(A) Aircraft

The SH-2G(A), shown in Figure 5, is a 14,200 lbs maximum take-off weight medium helicopter, configured for multi-purpose maritime use. It is a twin-turboshaft engine, single main rotor and anti-torque tail rotor naval helicopter specifically designed for small ship operations. The SH-2G(A) is an upgraded version of the SH-2G, which initially entered service with the U.S. Navy in 1993. Additional versions of the SH-2G are in service with the Arab Republic of Egypt [SH-2G(E)] and in production for the Royal New Zealand Navy [SH-2G(NZ)].

The missions for the SH-2G(A) are surface surveillance; anti-surface warfare, anti-submarine warfare, contact investigation and counter infiltration; and utility support, which includes search and rescue operations, carriage of personnel and equipment, re-supply of ships at sea by vertical replenishment, and medical evacuation.

The helicopter is capable of operation from ANZAC class ships in recovery assist landing, free-deck and clear-deck operations, and from airfields and unprepared fields. The installation of the RAST probe for the recovery assist landing required modifications to the aircraft centre tub as described in the following section.

Figure 5. SH-2G(A) aircraft

3.2 Airframe Structural Modifications

As with the main rotor, the positioning of the RAST probe is most effective when located close to the centre of gravity of the aircraft. For the SH-2G(A) the probe is located in the centre tub section directly below the main rotor shaft. The centre tub consists of a deep keel beam (21 inches in depth) that runs on BL 0.00 from the nose back to Station 242 where it begins to taper to its end at Station 285. It divides the tub into two cells, with the left and right side skins and floor forming the rest of the box. The fuel is contained in the centre tub by bladder tanks located in the tub box cells between Stations 118 and 214.

The RAST probe is located on the underside of the aircraft just to the right of the keel beam between Stations 176 and 188. It is supported by a lower fitting at the skin level and an upper fitting at the floor level. The fittings are encased in a sheet metal box that extends from the floor to the skin where the crashworthy fuel cells were designed around the RAST probe support box. Figure 6 shows the RAST probe support structure.

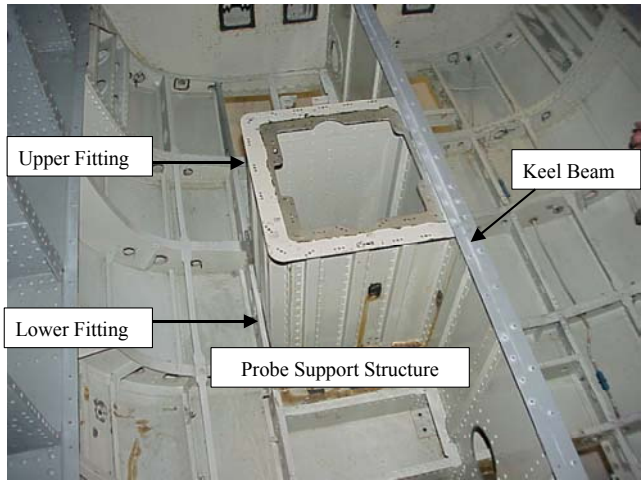

Figure 6. SH-2G(A) probe support structure, floor removed – looking aft

The lower support fitting reacts 100% of the probe downward load and approximately 190% of the loads applied in the fore or aft and lateral directions at the tip of the probe (Figure 7). The

190% factor is due to the fact that the probe tip extends 18 inches below the lower fitting and all of the bending moment on the probe is taken out as a couple. This couple is reacted at the lower fitting at the fuselage skin level and at the upper fitting located some 20 inches above it at the floor level.

The lower fitting is fastened directly to the fuselage skin. The basic load path for the in-plane loads (fore/aft and lateral) is bearing in the probe bore ring reacted by a fastener pattern into the 0.063 aluminum skin with the overturning moment taken out through integral ribs out to the frames at Stations 176 and 188 and the keel beam. The basic load path for the out-of-plane load (vertical) is bearing on a flange integral to the lower portion of the probe bore ring. The ring then distributes this downward bearing pressure load and reacts it in a gimbal ring fashion out to the four edges of the fitting box through the four ribs that act as trunnions to this gimbal ring. The load is then carried by the two frames and the keel beam.

The envelope that is used by the probe system is roughly a 12 by 12 by 20 inch cube going from the bottom of the fuselage to the floor. The side walls enclosing this cavity are designed to withstand the fuel pressures. To carry this pressure two hat sections are required per panel side (3/4 inch deep and .040 thick). These hat sections span from the floor to the inner cap of the frames where the hat sections are riveted. The upper fitting is attached directly to the underside of the floor. This fitting carries only in-plane loads (Figure 7). Loads introduced from the upper flange of the probe are supported by the upper fitting, which is attached to the upper keel cap and floor. The floor is of honeycomb construction with a 0.016 aluminum facing that is increased locally by a 0.025 doubler, which is co-cured in the assembly of the floor panels.

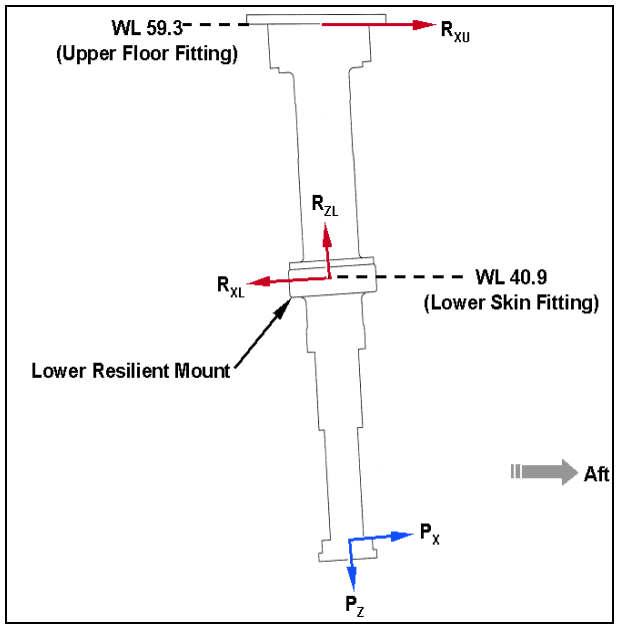

Figure 7. Probe forces and reactions

4 Structural Analysis

4.1 Finite element analysis of the probe design

The securing loads from dynamic simulation of the aircraft system were used for the structural analysis of the helicopter probe and housing [6]. The probe assembly is essentially cantilevered from the airframe with the interface between the probe and housing formed by resilient material. This created a structural challenge to determine the correct load path and boundary conditions for stress analysis. Four finite element analysis (FEA) models were used to analyze various structural behaviours. One model was used to study the load transfer between the probe and the housing. Another was used for studying similar action between the probe and load contact area (the crenellated ball located at the outboard end of the probe). The other two models were used for detailed study of the housing and the top flange/airframe interface. Other probe components required only a single FEA model for analysis.

Figure 8 presents a typical FEA model of the probe shaft and housing indicating magnified probe deflection as the result of tip loading.

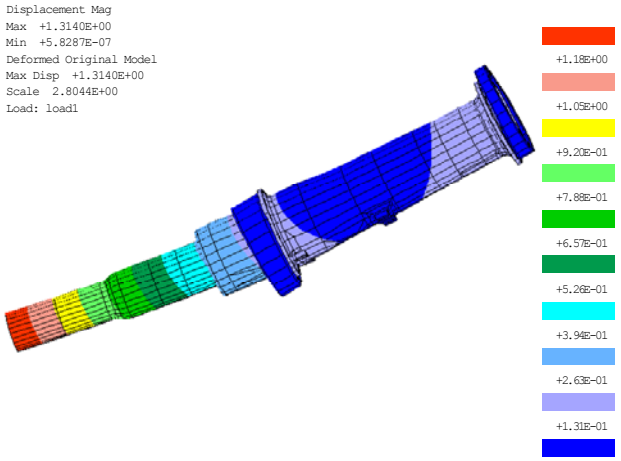

Figure 8. FEA model of the probe shaft and housing indicating magnified probe deflection

4.2 Finite element model and analysis of aircraft structure

The SH-2G airframe finite element model was modified to represent the probe support structure for the SH-2G(A). The skin, stringers, keel, frames, and probe support fittings of the centre tub were modelled in sufficient detail to obtain internal loads for analysis. The model is a modified version of the SH-2G model that was used by KAC and accepted by the US Navy for analysis when the aircraft was converted from an SH-2F to an SH-2G. The centre tub modifications were constructed using MSC Patran as a pre-processing tool. The analysis was conducted using MSC Nastran as the finite element solver. Critical load conditions were evaluated using graphic displays of stress contour plots. Internal loads were then extracted from the model using KAC-developed post processing scripts in conjunction with Patran.

Following the static tests of the probe installation, model results were compared with test results and shown to be in good agreement within statistical scatter bounds.

5 Experimentation

5.1 Proof load testing of the probe

Proof load testing was conducted to verify the probe structural design and validate the finite element models. The finite element results were used to select appropriate strain gauge positions for use in testing. The critical stress area for the probe was the contact area between the probe and the housing. Unfortunately, it was not accessible for strain gauging. Consequently, alternative high stress areas on the outside of the housing were chosen for strain gauge application. The probe passed proof load testing and good correlation was obtained between the test results and the FEA models.

5.2 Fatigue testing of the probe, housing, and supporting structure

Fatigue testing of the probe, housing and supporting structure was performed in a single fatigue test of an advanced development model (ADM) probe which was performed to failure to identify the mode of failure and also to obtain data to calibrate a generically-shaped component S-N curve for the probe. For the test, the ADM probe was mounted in ITI's hydraulic load test cell as shown in Figure 9. A fitting was developed for the probe tip that transmitted loads to the probe in a manner similar to the actual RSD.

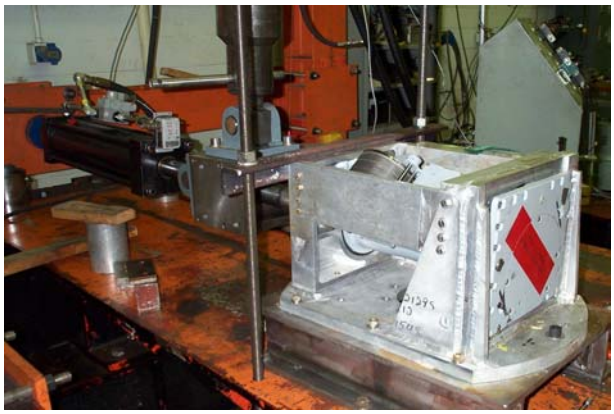

Figure 9. Probe and housing undergoing fatigue test in ITI's hydraulic load test cell

A progressively increasing block loading approach was used to define the lateral applied load amplitude as a fraction of the load that would produce ultimate stress in the probe system. The lateral load corresponding to ultimate stress in the aluminium and steel probe components was determined from the finite element stress analysis results [6] and the lower of the two values was used to determine the experimental loading. During testing, fully reversed loading (R = -1) was used for the primary lateral loading. Vertical loads were applied simultaneously with the primary lateral loading with a load double amplitude equal to 1/3 of the lateral load amplitude. This ratio, based on the dynamic analysis results, was selected as a conservative representation of the secondary vertical probe loading. A combination of inspection between loading blocks and automated measurement of the applied force and resulting probe tip deflection was used to identify the time and mode of failure of the probe.

The number of load cycles applied as a function of load amplitude prior to probe fatigue failure is reproduced in Table 3. $F_{ultimate}$ used for determining test loading was 19,500 lbf lateral based on results from the dynamic analysis. The number of applied load cycles per load level closely agrees with the 5000 specified in the test procedure for load levels up to 74% of $F_{ultimate}$. Partly through the 80% load level it was determined analytically that the probe fatigue test had demonstrated that the probe had conservatively exceeded its fatigue design requirements. Due to scheduling restraints and availability of the fatigue test equipment, it was jointly agreed by ITI and KAC to discontinue cycling (after 1747 cycles) at the 80% load level and proceed to load cycling at a 90% load level to obtain expeditious failure that was the intent of the accelerated fatigue test. Fatigue failure of the probe occurred after 729 cycles at 90% of $F_{ultimate}$.

Table 3. Load cycles applied during the probe system fatigue test prior to failure

% of $F_{ultimate}$	Actual cycles
50	5022
56	5018
62	5015
68	5000
74	5001
80	1747
90	729

The mode of failure of the probe was fatigue failure of the aluminium upper flange portion of the probe assembly as indicated in Figure 10.

Figure 10. View of the aluminum upper flange indicating the expected mode of probe system fatigue failure

Knowing the point of failure and the sequence of fatigue test loading provided sufficient information to iteratively calibrate a generalized component S-N curve. Figure 11 shows the results of the component S-N curve calibration based on the fatigue test results. The solid line labelled ‘standard S-N curve’ is the generalized component S-N curve corresponding to locations with high stress concentrations. The results of the fatigue test (Table 3) were used as a guide for shifting the standard curve to the right such that the known failure point lies on the S-N curve. The resulting curve is indicated by the dotted line labelled ‘failure S-N curve’. Palmgren-Minor cumulative damage analysis verified the correctness of this curve. The cumulative damage resulting from the test data

and the determined curve (dotted line) equalled 1, as it should knowing that a fatigue failure occurred. Next, based on the safe life approach, the dashed curve labelled 'safe life S-N curve' was defined where the number of cycles was reduced to ¼ of those associated with the failure curve. This component safe life curve was subsequently used for cumulative damage analysis of the probe system.

Palmgren-Minor cumulative damage analysis was performed combining the results of the dynamic interface analysis with the calibrated safe-life S-N curve.

The results of the analysis showed that for the SH-2G(A) specified operating profile, the predicted safe life of the probe system greatly exceeds the 30-year design life for fatigue and consequently fatigue failure of the probe is not expected. The results confirmed that probe design is governed by the peak static loads that are experienced during severe operating conditions and not by fatigue, as the vast majority of load cycles that occur in service are of much lower magnitude than the peak static loads the system must be able to withstand. A noteworthy feature of the fatigue analysis is that the resulting fatigue analysis report [7] is formulated such that the fatigue life estimate can be updated for different aircraft operating profiles should in-service conditions change over the course of the aircraft life.

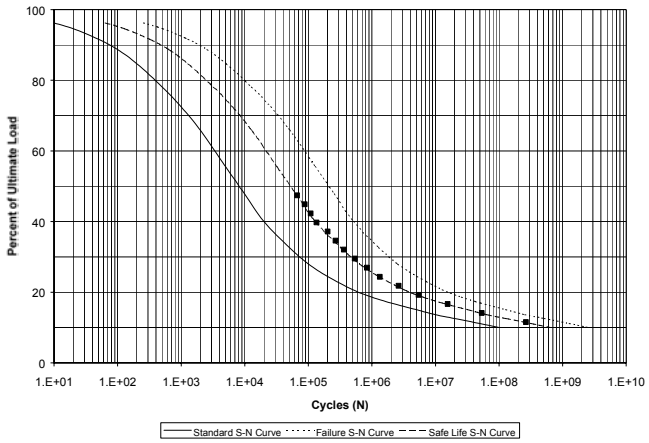

Figure 11. Cycles to failure versus load amplitude curves for the probe

5.3 Static and fatigue testing of the airframe

Static and fatigue tests with the RAST probe installed in the airframe were conducted. Static tests were conducted to 105% ultimate load to demonstrate structural integrity of the airframe support structure. Fatigue testing was conducted to a determined number of cycles at a load level demonstrating two lifetimes of service usage. Fatigue testing of the airframe was conducted first, followed by the limit and ultimate static tests.

The fatigue test set-up is shown in Figure 12. As with the probe, the damaging fatigue loads for the airframe occur when the probe is loaded in the vertical and lateral directions. Loads in the fore/aft direction due to aircraft pitching are generally lower due to the larger wheelbase between the probe and landing gear as compared to the lateral probe loading where the distance between the probe and the landing gear is smaller. Therefore, the fatigue testing loaded the aircraft with alternating loads in the vertical and lateral directions as shown in Figure 12.

The test loads and number of cycles were determined based on the results of the dynamic interface study conducted by ITI [4]. Based on this analysis, load conditions were lumped into 12 cases, as described in Reference 8, which considered sea state conditions, ship headings, aircraft alignment on the deck, aircraft gross weight, wind speed and wind direction. For each case 18 bands of loading in the lateral direction were specified with increasing levels of alternating load. The bands started at 500 lbs and increased 500 lbs for each band. Considering each band of loading, a damage fraction was determined by combining the cases with the appropriate cycle count. Using Miner's rule a total damage fraction was calculated and a mean fatigue life of 6.62 service lifetimes for the probe airframe support structure was estimated. A test load demonstrating 2 service lifetimes was then calculated using the results of the damage analysis. The final loading was a combined lateral/vertical alternating load of 5,200 lbs applied for a total of 13,900 cycles.

The testing was successfully completed demonstrating 2 service lifetimes of usage with no failures of the airframe support structure.

The static testing of the probe installation followed the completion of the fatigue tests. Static limit and ultimate loads as specified in the air vehicle specification were applied to the RAST probe installation. These loads successfully demonstrated the structural integrity of the aircraft backup structure for the upper sea state limited ship headings as defined in the air vehicle specification. The critical condition consisted of a combined loading in the vertical, lateral, and fore/aft directions, where the predominate loading consisted of loads applied in the vertical direction (22,000 lbs ultimate). The applied probe loads for this test were reacted by loads applied at the main and tail landing gear, engines, main gearbox, and various other mass items throughout the airframe. The test successfully achieved 105% ultimate loading with no failure or permanent deformation of the airframe support structure.

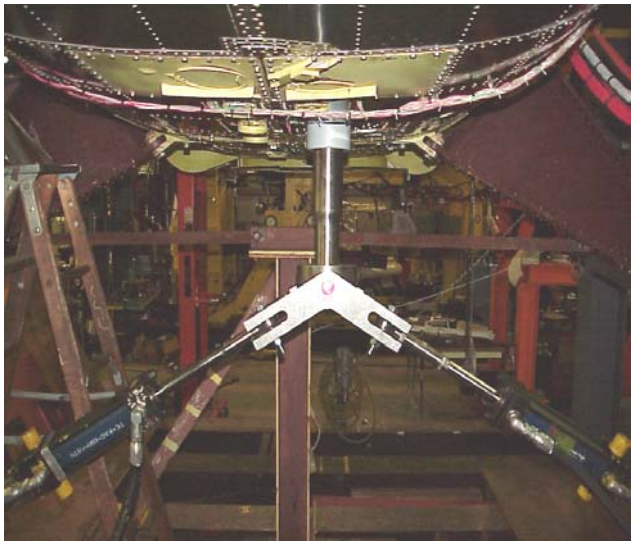

Figure 12. SH-2G(A) RAST Probe LCF Test, Looking Aft

5.4 Operational flight and ground testing of the probe installation

KAC performed approximately 35 hours of RAST ground testing and 8.8 hours of RAST flight testing using the SH-2G(A) helicopter (Figure 13). The purpose of the testing was to demonstrate operational functionality and compatibility with the RAST Deck Landing System. During these tests the aircraft was required to verify the ability to conduct recovery-assisted and free-deck landings into the RSD, to evaluate manoeuvring and straightening procedures once the aircraft was secured to the flight deck, and to demonstrate traversing operations needed to move the aircraft to and from the hangar.

The testing took place at KAC in Bloomfield, CT and the Naval Aviation Warfare Center (NAWC) Elevated Fixed Platform (EFP), Lakehurst, NJ from 26 October to 2 November 2000. Ground tests evaluated RAST probe cable functions, tension release, aircraft loads and mechanical stability while secured in the RSD. Aircraft configuration began at a GW of 12,066 lbs, and increased incrementally to approximately 14,016 lbs.

Figure 13. SH-2G(A) Aircraft in the RSD During Operational Testing.

As tested, the RAST system proved to be compatible with the SH-2G(A) aircraft with minor modifications. Configured with external stores, aircraft clearances and loading were satisfactory during landing and straightening evolutions. After H-2 line-up references were determined, modified Seahawk S-70B-2 straightening and traversing procedures were successful. Flight operations with the Recovery

Assist (RA) cable attached to the probe were evaluated at various aircraft gross weights and cable tensions.

6 Conclusion

A methodology combining dynamic interface analysis, detailed structural analysis and validation, and full-scale static and fatigue testing was developed and implemented to structurally substantiate the installation of the Indal Technologies Inc. RAST securing system in a Kaman SH-2G(A) Super Seasprite helicopter. The substantiation demonstrated a minimum of 2 lifetimes of service usage using loads that meet or exceed the air vehicle operational requirements for shipboard launch and recovery in severe sea conditions. While the application of this novel approach is specific to this application, the safe life methodology demonstrated herein is well suited to other safety-critical applications.

Acknowledgement

The dedicated effort of individuals at both ITI and KAC who contributed to the development and implementation of the methodology presented in this paper is gratefully acknowledged.

References

[1] Langlois RG and Tadros A. *User's manual for the aircraft/ship dynamic interface simulation DYNAFACE*. ITI Report 98-342, Indal Technologies Inc., 1998.

[2] Lloyd ARJM. *Seakeeping: Ship Behaviour in Rough Weather*. A.R.J.M. Lloyd, United Kingdom, 1998.

[3] Military Agency for Standardization. *Standardized wave and wind environments and shipboard reporting of sea conditions*. Standardization Agreement 4194, North Atlantic Treaty Organization, April 1983.

[4] *Dynamic interface study to investigate the peak securing forces for Kaman SH-2G(A) aircraft operation on the RAN ANZAC and OPC Vessels*. ITI Report 97-332, Indal Technologies Inc., 1997.

[5] *Annual Book of ASTM Standards*. Vol. 3.01, E1049-85 Standard practices for cycling counting in fatigue analysis, pp 707-15, 1997.

[6] *Kaman probe assembly structural design report*. ITI Report 97-334 Rev. A. Indal Technologies Inc., 1998.

[7] *Fatigue analysis report for Kaman SH-2G(A) aircraft probe*. ITI Report 98-373, Indal Technologies Inc., 1998.

[8] Langlois R, Moquin D and Rocconella B. *Consideration of the effect of securing and traversing loads on the fatigue life of the Kaman Seasprite RAST/ASIST probe installation*. In Proceedings of AHS Forum 55, Montreal, Canada, May 1999.

CURTISS-WRIGHT

Info

curtisswrightds.com

Email

ds@curtisswright.com